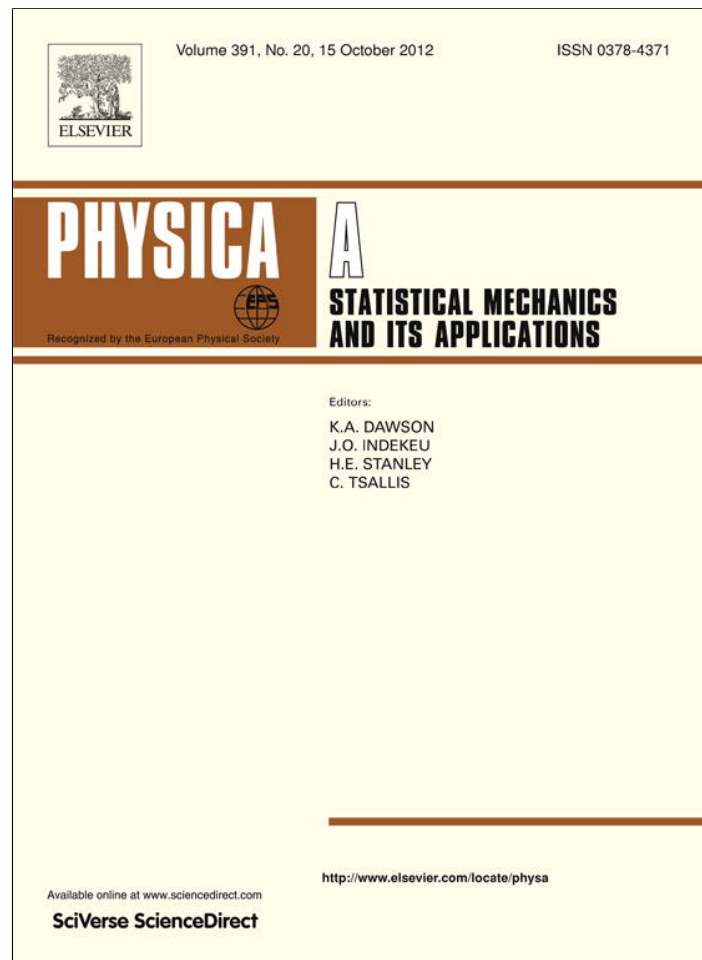


Provided for non-commercial research and education use.
Not for reproduction, distribution or commercial use.



This article appeared in a journal published by Elsevier. The attached copy is furnished to the author for internal non-commercial research and education use, including for instruction at the authors institution and sharing with colleagues.

Other uses, including reproduction and distribution, or selling or licensing copies, or posting to personal, institutional or third party websites are prohibited.

In most cases authors are permitted to post their version of the article (e.g. in Word or Tex form) to their personal website or institutional repository. Authors requiring further information regarding Elsevier's archiving and manuscript policies are encouraged to visit:

<http://www.elsevier.com/copyright>



Contents lists available at SciVerse ScienceDirect

Physica A

journal homepage: www.elsevier.com/locate/physa

Universal scaling behaviors of meteorological variables' volatility and relations with original records

Feiyu Lu^a, Naiming Yuan^a, Zuntao Fu^{a,*}, Jianguyu Mao^b

^a Lab for Climate and Ocean-Atmosphere Studies, Department of Atmospheric and Oceanic Sciences, School of Physics, Peking University, Beijing, 100871, China

^b LASG, Institute of Atmospheric Physics, CAS, Beijing, 100029, China

ARTICLE INFO

Article history:

Received 14 April 2011
Received in revised form 5 March 2012
Available online 22 May 2012

Keywords:

DFA
Volatility
Nonlinearity

ABSTRACT

Volatility series (defined as the magnitude of the increments between successive elements) of five different meteorological variables over China are analyzed by means of detrended fluctuation analysis (DFA for short). Universal scaling behaviors are found in all volatility records, whose scaling exponents take similar distributions with similar mean values and standard deviations. To reconfirm the relation between long-range correlations in volatility and nonlinearity in original series, DFA is also applied to the magnitude records (defined as the absolute values of the original records). The results clearly indicate that the nonlinearity of the original series is more pronounced in the magnitude series.

© 2012 Elsevier B.V. All rights reserved.

1. Introduction

It is recognized that long-term persistence, characterized by the autocorrelation function $C(n) = \langle (x_{i+n} - \bar{x})(x_i - \bar{x}) \rangle / \sigma^2$ decaying as a power law $C(n) \sim n^{-\gamma}$ (where n is the time lag, \bar{x} denotes the mean value of the record, and σ^2 is its variance), is ubiquitous in Nature. One can characterize the long-term persistence by the power spectral density $S(f) = |x(f)|^2$, where $\{x(f)\}$, $f = 0, \dots, N/2$, is the Fourier transform of the records $\{x_i\}$. If $\{x_i\}$ is long-term correlated, $S(f)$ decays by a power law $S(f) \sim f^{-\beta}$, with $\beta > 0$ characterizing the long-term memory. It has been proved that both the autocorrelation function $C(n)$ and the power spectral density $S(f)$ can be applied to stationary time series equally with $\gamma = 1 - \beta$ [1–3]. However, for non-stationary records, such as temperature records characterized by additional warming trends, more developed methods are needed. Thus, many methods, such as detrended fluctuation analysis (DFA for short) [4,1,5,6], wavelet analysis [7], and detrended moving average analysis (DMA for short) [8–10] have been proposed during the last few decades. Due to its simplicity and reliability, DFA is one of the most widely used methods and has been applied in various fields, such as DNA sequences [4,11], heart rate dynamics [12], economic time series [13] and climate research [1,14–23]. The DFA exponent α is equal to the Hurst exponent measured by rescaled range (R/S) analysis, and takes a relation with γ as $\alpha = 1 - \gamma/2$ [1]. Obviously, due to different controlling mechanics, different kinds of variables often show different α , for example, $\alpha \sim 0.65$ for atmospheric temperature and daily maximum temperature [24,1,25], $\alpha \sim 0.75$ for relative humidity [26,27] and $\alpha \sim 0.8$ for sea surface temperature [17]. Furthermore, even the same variable with different time frequencies can show different scaling behaviors, for example, 10-minute temperature series have long-term correlations of 0.75, compared to 0.65 for daily temperature [28]. These different scaling behaviors can be helpful for our understanding of the controlling mechanics of different systems in Nature. Besides the studies of mono-fractal (or two-point long-term) correlations, more methods or ideas based on DFA have been developed, such as multi-fractal detrended fluctuation analysis (MFDFA for short) [29,30] for multi-fractal properties, detrended cross-correlation analysis (DCCA for short) [31–35] for long-term correlations between

* Correspondence to: School of Physics, Peking University, Beijing, 100871, China. Tel.: +86 010 62767184; fax: +86 010 62751094.
E-mail address: fuzt@pku.edu.cn (Z. Fu).

two non-stationary time series, and volatility/magnitude analysis for nonlinear properties. In this work, we mainly focus on volatility/magnitude analysis of the different climate variables.

The volatility of time series, usually defined as the magnitude of the increments between successive elements, has been widely studied in physical, biological and sociological systems [36–38], especially in the financial and stock markets, where the volatility indicates the price changes and is crucial in understanding market dynamics [39]. There are also models to simulate the properties of volatility series [28]. The long-term correlations in volatility series (represented by α_{vol}) are recognized to be influenced by the long-range correlations of the original series (represented by α), as well as the nonlinear or multi-fractal properties. Recently this concept has been applied to meteorological statistics. For some series characterized by strong long-term correlations with $\alpha > 1$, their volatility series show relatively strong correlations, in agreement with nonlinearity of the original records [40]. However, such long-range correlations in volatility series are difficult to determine for many meteorological time series such as daily temperature over land and soil moisture, with $\alpha_{vol} < 0.6$ (or $\alpha_{vol} \sim 0.6$ due to the selection of different time scales) [41–43]. There have been some simulations and analytical research on the relation between volatility and original series [40]. Previous research stated that as the nonlinearity of the original series increases, the correlations of the volatility series become stronger. This conclusion was then used to identify the nonlinear properties in temperature time series. However, in some other research the scaling behaviors of volatility and original series did not agree with this conclusion [42,43].

In this paper, we analyze the long-range correlations in the volatility series of five meteorological variables, including daily mean relative humidity, daily mean temperature, daily temperature range (DTR for short), daily maximum and minimum temperature over China. Although these are five different kinds of variable, unlike the different scaling behaviors for different kinds of original variable we mentioned above, the long-range correlations of all five variables' volatility series are similar, with α_{vol} all slightly above 0.5 (most are round 0.54), and the standard deviations are similar to each other. A further numerical test is made, which indicates a universal scaling behavior of the volatility series. Besides, we find that the scaling exponents of the volatility series do not have remarkable connections with the long-range correlations or nonlinear properties of the original series. However, for the magnitude series, which are further constructed by calculating the absolute values of the original records (with annual cycle removed for climate records), more pronounced relations between the magnitudes and the original records arise. More details will be shown in the following sections.

2. Methodology and data

2.1. Datasets

In this paper, the data we used were obtained from a high-quality daily surface climatic data set, processed by the Chinese National Meteorological Information Center (NMIC), of 194 Chinese meteorological stations taking part in international exchange. Our analysis is mainly based on 190 stations that have all the five different kinds of data, including daily mean relative humidity, daily mean temperature, daily temperature range, daily maximum and minimum temperature. The length of the records is about 50 years, from the 1950s to the 2000s. Since the length of the records is a little less than 20,000 days, the scaling range we choose is mainly from 30 to 1000 days.

For each meteorological series, we construct two kinds of series from the original series. The processes are shown in Figs. 1 and 2 as per the instructions below.

- (i) The volatility series $V_i = |x_i - x_{i-1}|$.
- (ii) The magnitude series of the fluctuations $F_i = |x_i - \langle x_i \rangle|$, where $\langle x_i \rangle$ is the climatological annual periodicity.

For brevity, we call V_i the volatility series and F_i the magnitude series. Then we remove the annual cycles of F_i and V_i separately, to obtain ΔF_i and ΔV_i . When obtaining the series of ΔF_i , it should be noticed that we removed annual cycles twice. The first time was to get the fluctuations out of the original series, which has a mean value of zero. The second time was to remove the remaining periodicity. The F_i series in Fig. 2 exhibits an annual cycle, proved by both standard Fourier tests and crossovers at the timescale of 1 year in the DFA results [44]. This residual periodicity can be easily understood since the fluctuation strength varies regularly in different seasons. To be clear, in the following sections we use volatility series for series (i) and magnitude series for series (ii).

2.2. Outline of the methodology

For a given series $x_i (i = 1, 2, \dots, N)$, the DFA method includes 5 steps [6].

- (i) We calculate the increments of x_i as its “profile”, which is given by integration as

$$y_j = \sum_{i=1}^j x_i, \quad j = 1, 2, \dots, N. \quad (1)$$

- (ii) The profile y_j is divided into $N_n (= [N/n])$ non-overlapping windows of equal length n . The same process is performed from the end of the series to the beginning to take account of the remaining data after N_n windows.

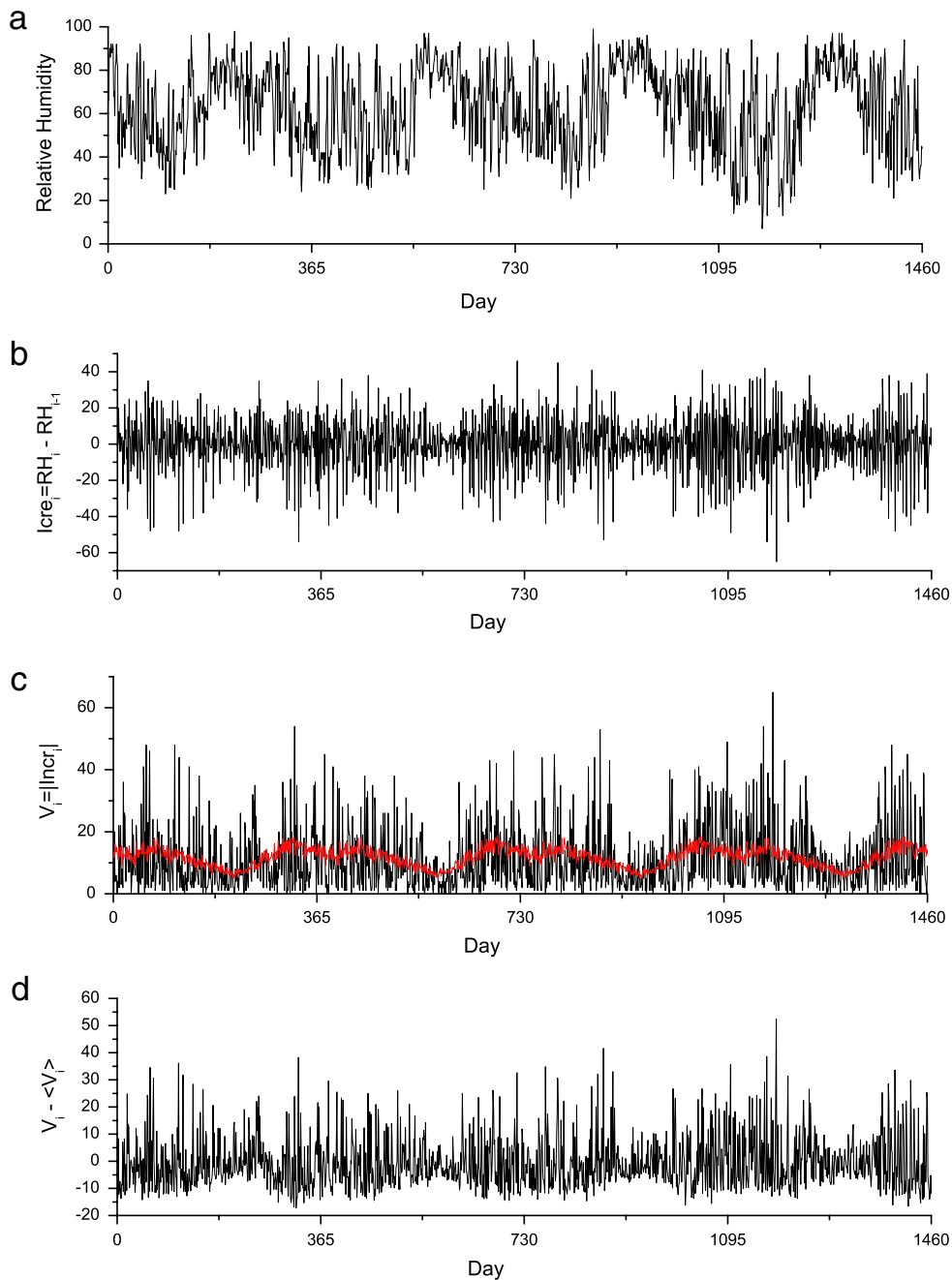


Fig. 1. The process of obtaining series (i). (a) Four years (out of 51) of relative humidity series for Station 54511. (b) The increments of relative humidity series in (a). (c) The magnitude series of the increments in (b) and its annual cycle (red). (d) The final volatility series of relative humidity. (For interpretation of the references to colour in this figure legend, the reader is referred to the web version of this article.)

(iii) In every window, the local trend is fitted by a polynomial function $f_p(j)$ of order p and the profile is detrended by subtracting local fitted functions:

$$y'_j = y_j - f_p(j), \quad j = 1, 2, \dots, N. \quad (2)$$

In this paper, we used DFA-3, which means that we used polynomial functions of order-3 in this step. As shown in Fig. 3, it is clear that DFA-3 is enough to eliminate quadratic trends in meteorological time series and DFA of higher order has little influence on the results of the analysis [6]. However, some other trends or periodicities may have some influence on the results [44], and Ref. [35] is a good review for details.

(iv) In order to use all the elements in the series, we take N_n windows backward from the end of the series. Then we calculate the variance within each of the $2N_n$ windows:

$$F_n^2(j) = \frac{1}{n} \sum_{i=1}^n y_j'^2 [(j-1)n + i]. \quad (3)$$

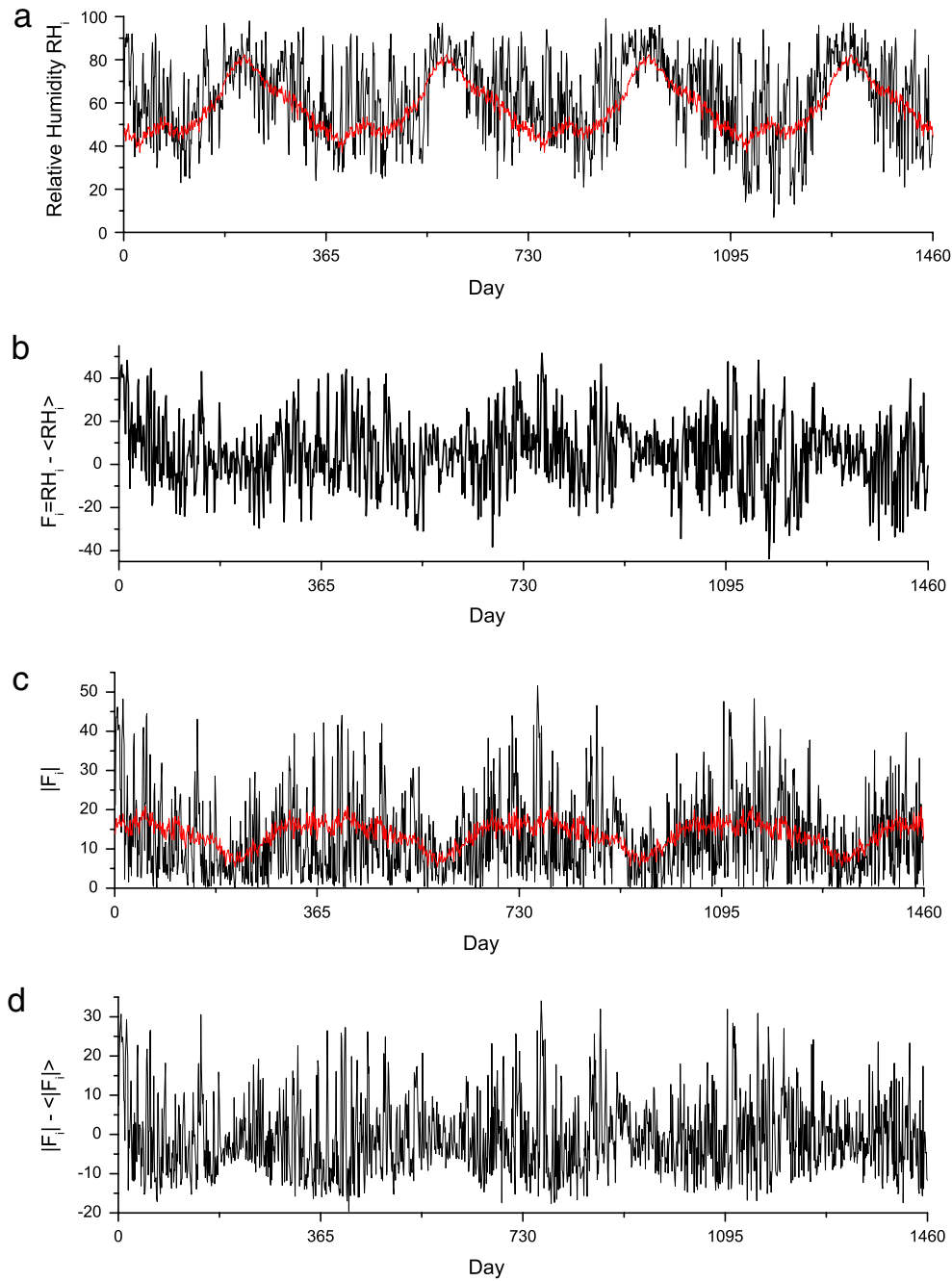


Fig. 2. The process of obtaining series (ii). (a) Four years' data (out of 51) of relative humidity series for Station 54511 (Beijing) and the climatological cycle (red). (b) Relative humidity fluctuations after the removal of the climatological cycle. (c) The magnitude series of the relative humidity fluctuations in (b) and its annual cycle (red). (d) The final magnitude series of fluctuations with the annual cycle removed. (For interpretation of the references to colour in this figure legend, the reader is referred to the web version of this article.)

(v) The DFA fluctuation function is calculated as the square root of the average variance of all windows, using the variances we get in Eq. (3), as

$$F(n) = \sqrt{\frac{1}{2N_s} \sum_{j=1}^{2N_s} F_n^2(j)}. \quad (4)$$

If the series has long-range correlations, then $F(n)$ and n have a power-law relationship

$$F(n) \propto n^\alpha \quad (5)$$

with scaling exponents α as the indication of long-range correlations. The $F(n) \sim n$ line can be drawn on a double logarithmic graph, and the scaling exponents can be obtained as the slope of the line. For uncorrelated time series, $\alpha = 0.5$. Long-range correlated series have DFA exponents $\alpha > 0.5$ while $\alpha < 0.5$ is for long-range anti-correlated processes.

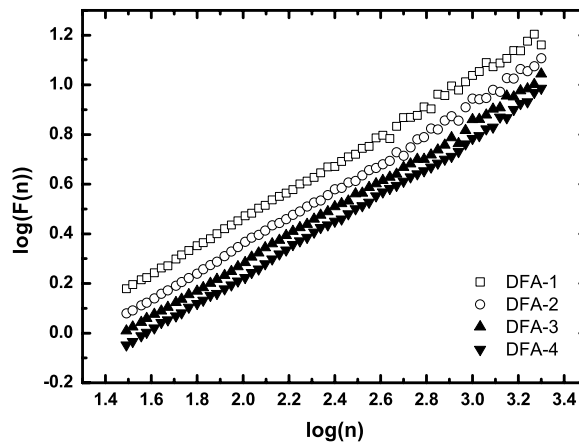


Fig. 3. Representative results of DFA-1, DFA-2, DFA-3, and DFA-4. The time series analyzed are magnitude series obtained from Station 50527 (Hailaer), which was selected randomly. One can see that DFA-3 is sufficient to get reliable results.

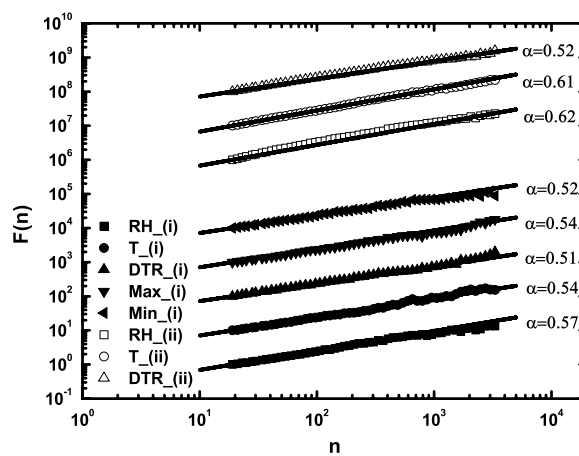


Fig. 4. DFA-3 results of volatility (lower full symbols) and magnitude (upper open symbols) series for Station 54511 (Beijing). The curves are shifted by a factor of 10. (RH for relative humidity, T for temperature, DTR for daily temperature range, Max for daily maximum temperature and Min for daily minimum temperature.)

For volatility series, we chose all 190 stations that have five data series since the $F(n) \sim n$ curves are all straight and the time interval is [30, 1000] days. When analyzing the DFA-3 exponents of the original series and magnitude series, we selected the stations with $F(n) \sim n$ curves of good linear fit in the intervals we chose (163 stations for daily relative humidity in [100, 1000] days, 176 stations for daily temperature range and 167 stations for daily mean temperature in [100, 700] days).

In order to investigate the effects of the nonlinearities in the original series on the magnitude series and volatility series, we applied the surrogation method of iAAFT to the relative humidity series, which effectively destroys higher order correlations and cross-correlations between the two series [45], while not affecting 2-point correlations in the series [46]. Then we got the surrogate series for the (i) and (ii) series from their original series and applied the DFA method to them as well. The results of surrogation will be shown in the next section.

3. Results

Fig. 4 shows the DFA results for the volatility series (represented by (i)) and the magnitude series (represented by (ii)) for Station 54511 (Beijing), with 5 variables for series (i) (lower full symbols) and 3 for series (ii) (upper open symbols), respectively. All five lines for series (i) are close to straight lines with slopes between 0.51–0.57 within the whole time interval, [20, 3300] days. However, the DFA lines for series (ii) are not as straight as those of series (i) and the DFA exponents are expanded into a wider range, which is observable in the statistical data for all stations. However, there are no obvious crossovers in the lines of Fig. 4.

To look into the scaling patterns of series (i), Fig. 5(a)–(e) shows the histograms of the DFA-3 exponents for the five different meteorological variables from 190 stations. The five distributions all pass the Anderson–Darling normality test at 5% significance [47,48], thus they can be regarded as being drawn from normal populations. Their mean values, standard deviations and other statistics are shown in Table 1, where we can see that all the five different variables show weak long-term correlations with the mean α around 0.54. In order to prove that the α values we obtained (slightly higher than 0.5)

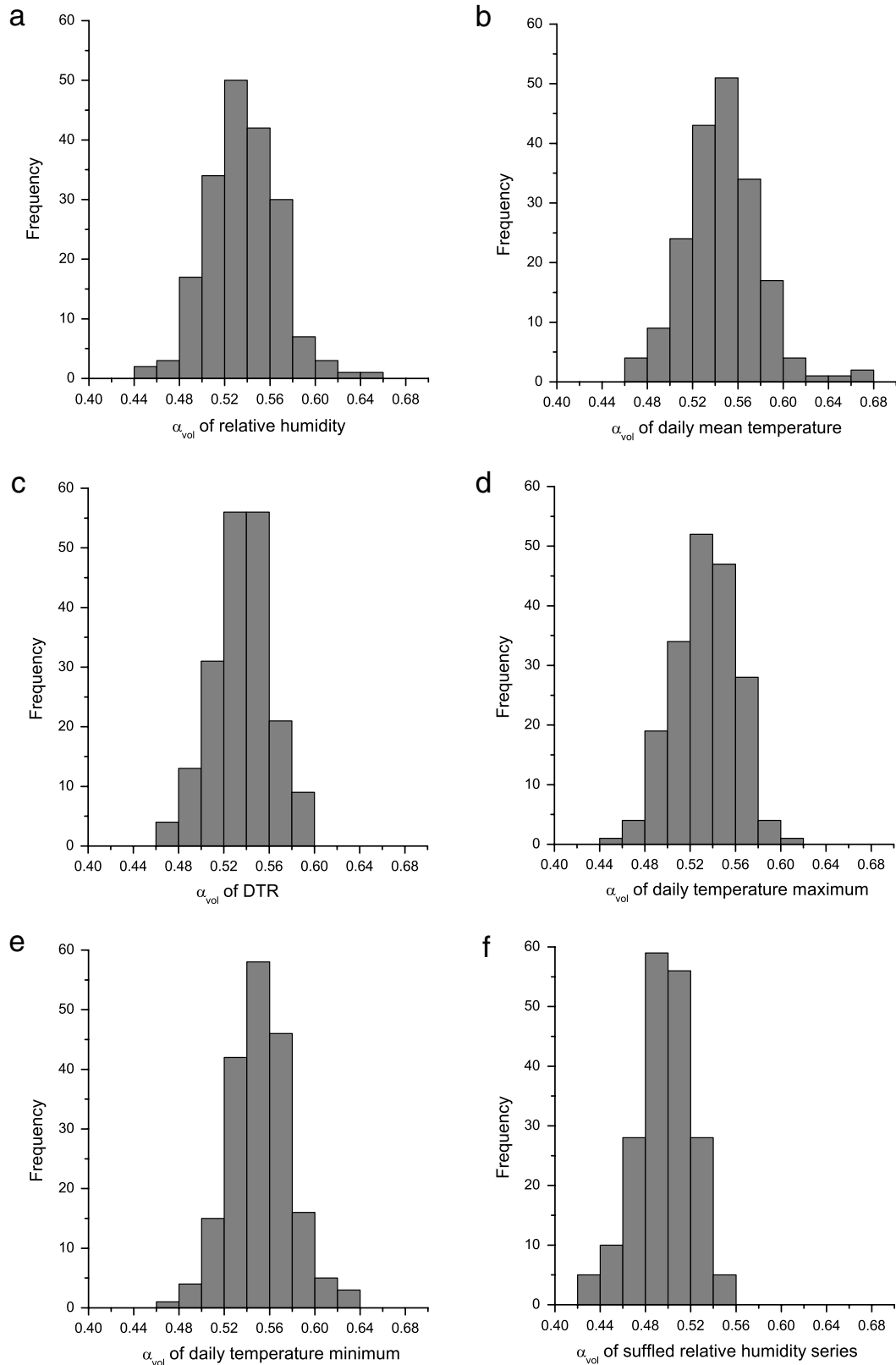


Fig. 5. The distributions of the volatility series' DFA-3 exponents for (a) relative humidity; (b) daily temperature mean; (c) daily temperature range; (d) daily temperature maximum; (e) daily temperature minimum; (f) shuffled relative humidity. All results include 190 stations over China.

are due to the variables' long-term correlations, rather than noise, we randomly shuffled the relative humidity series before obtaining the volatility series. It can be seen from Fig. 5(f) that the DFA-3 exponents for shuffled volatility series have mean value close to 0.5 (see also Table 1, bottom row). Thus we propose that the volatility series of the data we analyzed all have weak long-range correlations with similar strength.

Table 1

Statistical results for the distributions of scaling exponents in Fig. 5(a)–(f), and also for the scaling exponents obtained from the synthetically generated data.

| | Mean | Standard deviation | Max | Min | Median |
|---------------------------------|-------|--------------------|-------|-------|--------|
| Relative humidity | 0.537 | 0.032 | 0.656 | 0.444 | 0.556 |
| Daily mean temperature | 0.546 | 0.033 | 0.669 | 0.460 | 0.558 |
| Daily temperature range | 0.536 | 0.025 | 0.598 | 0.464 | 0.517 |
| Daily maximum temperature | 0.533 | 0.027 | 0.602 | 0.455 | 0.539 |
| Daily minimum temperature | 0.552 | 0.027 | 0.637 | 0.480 | 0.535 |
| Shuffled relative humidity | 0.496 | 0.025 | 0.560 | 0.429 | 0.528 |
| Artificial data $\alpha = 0.55$ | 0.549 | 0.023 | 0.637 | 0.466 | 0.549 |
| Shuffled artificial data | 0.499 | 0.022 | 0.576 | 0.415 | 0.499 |

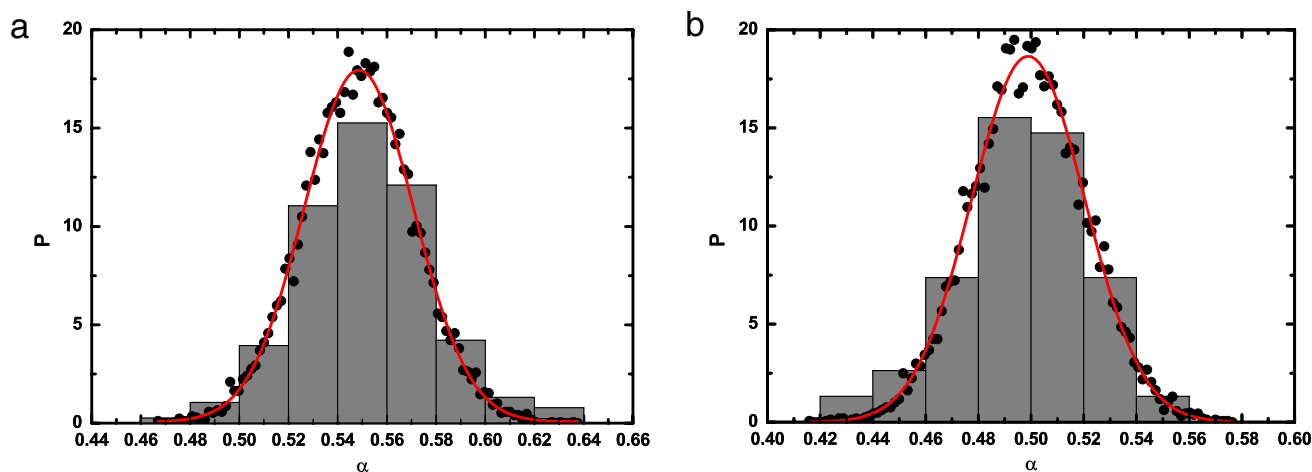


Fig. 6. Probability density of α obtained from the 10 000 synthetic long-term correlated (a), and shuffled (b) sub-records (black full circles and red curves). The histograms represent the averaged probability density in bins of size 0.02 for the α values obtained from the volatility series of the minimum temperature records (a), and the shuffled relative humidity records (b).

These weak correlations were also found in previous research for temperature and soil moisture data [41–43]. Govindan et al. looked into the volatility of daily maximum temperature series of 10 sites around the globe, and found that they all have $\alpha \sim 0.6$. Bartos did similar work, with over 7000 stations around the world, and came out with average α slightly smaller than 0.6. One important conclusion from previous results is that the scaling exponents of the temperature volatility series have no obvious patterns of geographical distribution [41,42]. All these phenomena are confirmed by our results, while the volatility series for the other variables do not have geographical dependence either. Considering all the findings above, and taking the small range of α into account, we would like to propose that there may be a universal scaling behavior with α smaller than 0.6 in the volatility series of meteorological records. According to Ref. [49,22], DFA exponents can scatter tremendously if we obtain the sub-record from a long (e.g., with a length of 2 million) record characterized by an α (e.g., $\alpha = 0.55$). Thus, we further make a numerical simulation to test whether the scaling behaviors of the volatility records are universal or not. We use a modified Fourier filtering technique [50] and generate 200 signals of length $L = 2^{21}$ characterized by $\alpha = 0.55$ (according to the mean α value of the daily minimum temperature’s volatility series). Then 10 000 sub-records with length $L = 20\,000$ are extracted from these 200 long records and the DFA is applied. By choosing the same scaling range as we did above ([30, 1000]), 10 000 α values ranging from 0.47 to 0.64 are obtained (more details are shown in Table 1). Note that the minimum and maximum α for the daily minimum temperature volatility series are 0.48 and 0.64, respectively; it is clear that the small α range indicates a universal scaling behavior. It can be seen from Fig. 6(a) that the black full circles denote the probability density function (Pdf for short) P of the 10 000 α values obtained from the numerical test. For better illustration, all the black points are fitted by the red curve. The histograms, which have the same shape as Fig. 5(e), represent the averaged probability density in bins of size 0.02 (e.g., 0.46–0.48, 0.48–0.50, etc.) for the α values obtained from the volatility series of the minimum temperature records. More clearly, the shapes of the histograms are roughly the same as the red curve, which can be an important hint to confirm the universal scaling behavior of the volatility series. Similar results can also be found for the other four different variables, thus we do not show the figures here. To further confirm our findings, we shuffle the 10 000 sub-records and repeat the calculations, see Fig. 6(b). Compared with the probability density of the α values for the shuffled volatility series (similar shape to that shown in Fig. 5(f)), as expected, the numerically simulated red curve also shows similar behavior (more details are shown in Table 1). The universal scaling behavior here may suggest that the volatility series from meteorological variables may be controlled by some universal atmospheric variability or stochastic process.

Next we study the relations among the original long-term correlated records, the volatility series, and the magnitude series. The relations between the long-range correlated time series and its volatility have been studied before by Kalisky

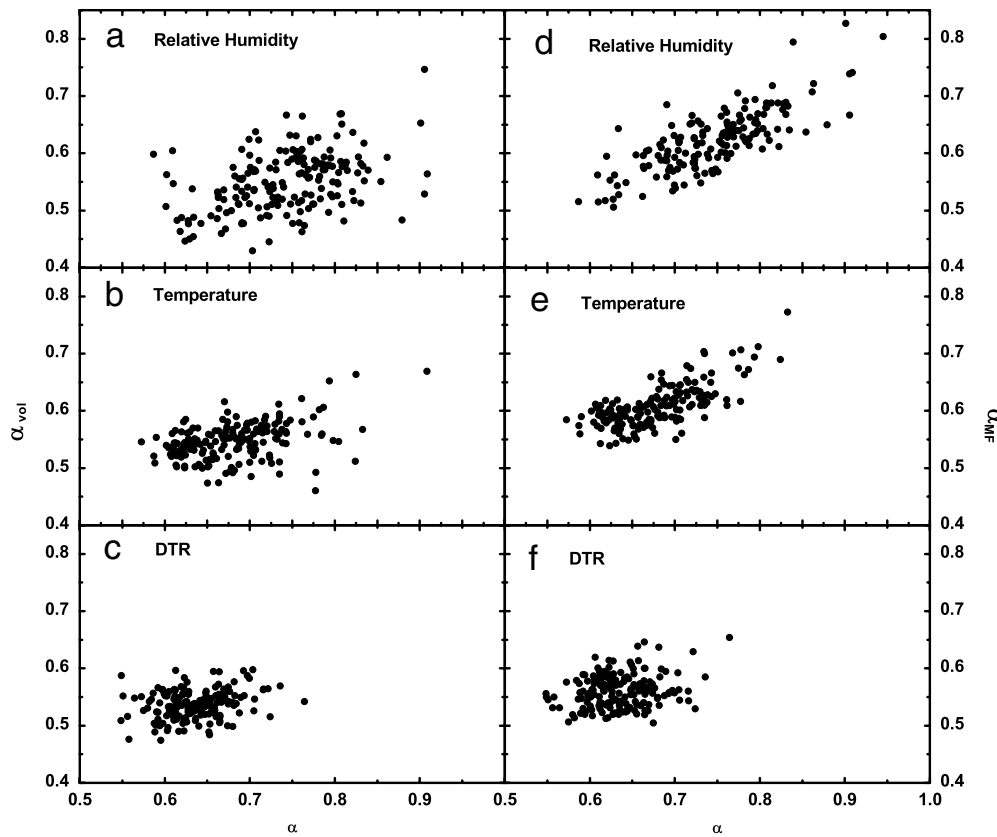


Fig. 7. Scatter plots of the DFA-3 exponents obtained from the original series as the x-axis, and obtained from the volatility series (left hand side) and the magnitude series (right hand side) as the y-axis. (a,d) relative humidity, (b,e) daily mean temperature, and (c,f) DTR.

et al. [40] and Podobnik et al. [28]. It is reported that the correlations in volatility are linked to the scaling behavior, especially the nonlinear properties of the original series. Following this work, we make three scatter plots between the scaling exponents of the volatility and the original series in Fig. 7(a)–(c), for relative humidity, daily mean temperature and DTR, respectively. We find that the DFA-3 exponents of the volatility are rather dispersed regardless of the exponents of the original series. These results do not follow the conclusion that $\alpha_{vol} \sim 0.5$ when $\alpha < 0.75$ and α_{vol} increases nonlinearly when $\alpha > 0.75$. There is no convergence of α_{vol} when α exceeds 0.8 in Fig. 7(a)–(c). In fact, the “volatility” used by Kalisky et al. was not the usual volatility we considered and the relations they have shown were actually about the original series u_i and the magnitude of its fluctuation $|u_i - \langle u_i \rangle|$ ($\langle u_i \rangle$ is the annual cycle of u_i as in Section 2.1), rather than its volatility series $|\Delta u_i|$. They implemented this “volatility” because the time series they generated were based on Gaussian white noise and were stationary per se with mean value of zero and finite variance. However, for the same original series u_i , these two series ($|u_i|$ and $|\Delta u_i|$) present significantly different statistical characteristics since we can regard u_i as the increment series of its profile series. So without obtaining the absolute values, the scaling exponents of u_i will be 1 larger than those of Δu_i . Thus we can say that the long-range correlations in the volatility series indicate the nonlinear correlations of the increment series rather than those of the original series. So we conducted similar calculations on the magnitude series (series (ii)) to test their relations with the original series.

Compared to Fig. 7(a)–(c), we can find apparent patterns between α (the DFA exponents of the original series) and α_{MF} (the DFA exponents of the magnitude series) in Fig. 7(d)–(f). The three graphs agree with each other, except that the points in the different graphs are located in different regions. We can see that α_{MF} stays around 0.6 before α reaches 0.75. In Fig. 7(f), the DFA-3 exponents of the original DTR series are all below 0.75 except for one station and the α_{MF} of 85% of stations range from 0.52 to 0.6. Fig. 7(e) also shows this similar pattern in its left part. Besides, α_{MF} increases linearly with α when α exceeds 0.75 (Fig. 7(d) and (e)). For the deep water temperature series T_i (which is characterized by α around 1) used in Ref. [40], its volatility series δT_i show strong long-range correlations with the DFA exponents of 0.72. However, most meteorological variables do not have such strong correlations as the deep water temperature.

In order to test how the nonlinearity of the original time series affects its magnitude and volatility series, we implemented the surrogating method of iAAFT [46]. This process destroys nonlinear correlations of the original series while maintaining 2-point correlations [45]. Fig. 8 shows the DFA results of the original and surrogated relative humidity series for Station 50353 (Huma) (a) and DTR series for Station 59758 (Haikou) (b). One can see that both figures show similar characteristics: the DFA curves of the original series and its surrogated series are almost parallel, resulting from the same 2-point correlations; however, the DFA curve of the surrogated magnitude series clearly has a smaller DFA exponent, compared to the magnitude series before surrogation. For the relative humidity (with 163 stations considered), the mean DFA-3 exponent of the

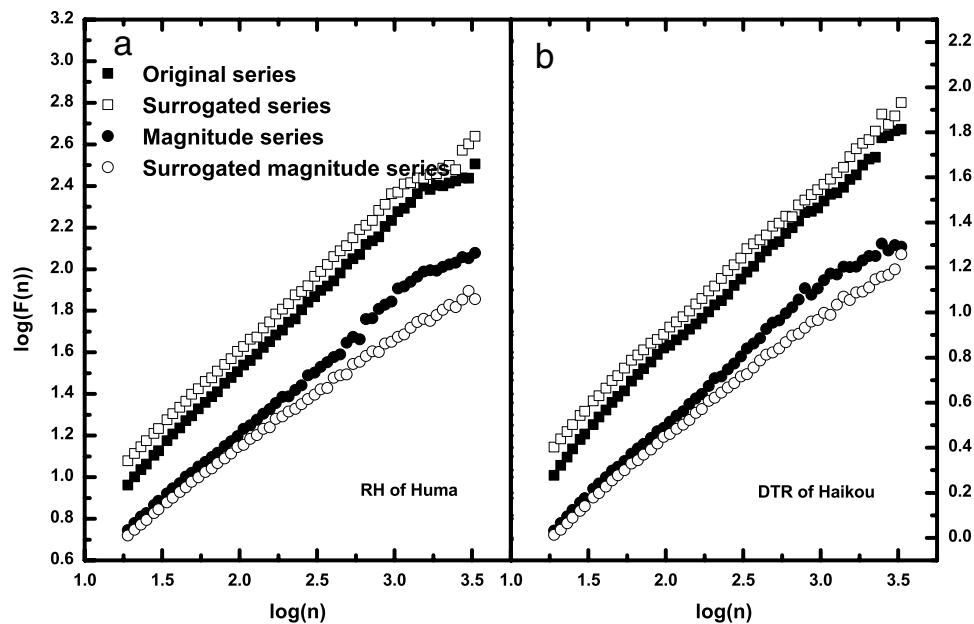


Fig. 8. DFA results of the original series, surrogated series, magnitude series, and surrogated magnitude series for relative humidity (50353, Huma, (a)) and DTR (59758, Haikou, (b)), respectively.

surrogated magnitude series is 0.05 smaller than that of the original magnitude series, and the DFA exponents of more than 90% of stations (150 out of 163) decreased after the surrogation. Thus the nonlinear properties of the original series do have impacts on the long-range correlations of the magnitude series. For comparison, we also applied the iAAFT surrogation to the process of analyzing the volatility series. However, since the volatility series only show weak correlations, the surrogating process did not have many effects on their DFA results. Most DFA exponents of the surrogated volatility series are still between 0.5 and 0.6; thus we cannot figure out how the nonlinearity of original series affects the correlations in its volatility series.

4. Conclusion and discussion

In this paper, the volatility series of different meteorological variables, including daily mean temperature, daily mean relative humidity, daily temperature range, daily maximum and minimum temperature are analyzed by means of DFA. We found that all the records have weak long-term correlations with similar strength. By making a numerical test and applying DFA to 10 000 sub-records of length $L = 20\,000$, we find that although the long records, which we extract the sub-records from, have identical long-term correlations, the DFA exponents obtained from the sub-records still scatter tremendously. The α range obtained from the numerical test is similar to (or even larger than) that obtained from the volatility series, which indicates a universal scaling behavior of the volatility series. In our opinion, this may mean that meteorological variables' volatility could be controlled by some universal atmospheric variability or stochastic process.

Compared to the universal scaling behavior of the volatility series, the magnitude series (series (ii) in Section 2.1) show better agreement with the nonlinear properties of the original series for relative humidity, daily temperature and temperature range series. We concluded that the nonlinear correlations of the original series are reflected in the magnitude series of their fluctuations, which have often been mixed up with the real volatility series and sometimes studied as volatility. It is also interesting to see long-range correlations in the volatility series of natural processes [40, Section IV.B]. This example just indicates that the magnitude of an anti-correlated series can be long-range correlated [28]. Thus we should be cautious when using scaling behaviors of volatility or magnitude series as indicators of nonlinear properties.

Nonlinearity is a crucial part in determining the statistical properties of natural process. Unfortunately, it is still difficult to identify whether a long-term correlated record only has linear properties or has both linear and nonlinear properties. The volatility series and magnitude series are both good indicators and their relations with the properties of the original series should be studied more quantitatively. However, this is much more difficult in the real environment than in theoretical analysis because of the extreme complexity in natural processes. Therefore these meteorological time series should also be considered from the basis of physical mechanisms and their scales, for example, how they are controlled by circulation systems, how the data are compromised by the process of averaging and how the static nonlinearity is affected by the measurement devices.

Acknowledgments

Many thanks are due for the support from the National Natural Science Foundation of China (Nos 40975027, 41175141) and from the Knowledge Innovation Program of the Chinese Academy of Sciences (IAP09301).

References

- [1] E. Koscielny-Bunde, A. Bunde, S. Havlin, H.E. Roman, Y. Goldreich, H. Schellnhuber, Indication of a universal persistence law governing atmospheric variability, *Phys. Rev. Lett.* 81 (1998) 729.
- [2] B.D. Malamud, D.L. Turcotte, Self-affine time series: I. Generation and analyses, *Adv. Geophys.* 40 (1999) 1.
- [3] S. Lennartz, A. Bunde, Distribution of natural trends in long-term correlated records: a scaling approach, *Phys. Rev. E* 84 (2011) 021129.
- [4] C.K. Peng, S.V. Buldyrev, S. Havlin, M. Simons, H.E. Stanley, A.L. Goldberger, Mosaic organization of DNA nucleotides, *Phys. Rev. E* 49 (1994) 1685–1689.
- [5] A. Bunde, S. Havlin, J.W. Kantelhardt, T. Penzel, J.H. Peter, K. Voigt, Correlated and uncorrelated regions in heart-rate fluctuations during sleep, *Phys. Rev. Lett.* 85 (2000) 3736.
- [6] J.W. Kantelhardt, E. Koscielny-Bunde, H.H.A. Rego, S. Havlin, A. Bunde, Detecting long-range correlations with detrended fluctuation analysis, *Physica A* 295 (2001) 441–454.
- [7] A. Arneodo, E. Bacry, P.V. Graves, J.F. Muzy, Characterizing long-range correlations in DNA sequences from wavelet analysis, *Phys. Rev. Lett.* 74 (1995) 3293.
- [8] E. Alessio, A. Carbone, G. Gastelli, V. Frappietro, Second-order moving average and scaling of stochastic time series, *Eur. Phys. J. B* 27 (2002) 197–200.
- [9] A. Carbone, G. Castelli, H.E. Stanley, Analysis of clusters formed by the moving average of a long-range correlated time series, *Phys. Rev. E* 69 (2004) 026105.
- [10] A. Carbone, G. Castelli, H.E. Stanley, Time-dependent Hurst exponent in financial time series, *Physica A* 344 (2004) 267–271.
- [11] S.V. Buldyrev, A.L. Goldberger, S. Havlin, R.N. Mantegna, M.E. Matsa, C.K. Peng, M. Simons, H.E. Stanley, Long-range correlation-properties of coding and noncoding DNA-sequences - genbank analysis, *Phys. Rev. E* 51 (1995) 5084–5091.
- [12] C.K. Peng, S. Havlin, H.E. Stanley, A.L. Goldberger, Quantification of scaling exponents and crossover phenomena in nonstationary heartbeat time-series, *Chaos* 5 (1995) 82–87.
- [13] Y.H. Liu, P. Cizeau, M. Meyer, C.K. Peng, H.E. Stanley, Correlations in economic time series, *Physica A* 245 (1997) 437–440.
- [14] P. Talkner, R.O. Weber, Power spectrum and detrended fluctuation analysis: application to daily temperatures, *Phys. Rev. E* 62 (2000) 150–160.
- [15] K. Fraedrich, R. Blender, Sfcaling of atmosphere and ocean temperature correlations in observations and climate models, *Phys. Rev. E* 90 (2003) 108501.
- [16] J.F. Eichner, E. Koscielny-Bunde, A. Bunde, S. Havlin, H.-J. Schellnhuber, Power-law persistence and trends in the atmosphere: a detailed study of long temperature records, *Phys. Rev. E* 68 (2003) 046133.
- [17] R. Monetti, S. Havlin, A. Bunde, Long-term persistence in the sea surface temperature fluctuations, *Physica A* 320 (2003) 581–589.
- [18] B. Podobnik, P.C. Ivanov, V. Jazbinsek, Z. Trontelj, H.E. Stanley, I. Grosse, Power-law correlated processes with asymmetric distributions, *Phys. Rev. E* 71 (2005) 025104.
- [19] D. Rybski, A. Bunde, S. Havlin, H. von Storch, Long-term persistence in climate and the detection problem, *Geophys. Res. Lett.* 33 (2006) L06718.
- [20] Xi Chen, Guangxing Lin, Zuntao Fu, Long-range correlations in daily relative humidity fluctuations: a new index to characterize the climate regions over China, *Geophys. Res. Lett.* 34 (2007) L07804.
- [21] D. Rybski, A. Bunde, H. von Storch, Long-term memory in 1000-year simulated temperature records, *J. Geophys. Res.* 113 (2008) D02106.
- [22] S. Lennartz, A. Bunde, Trend evaluation in records with long-term memory: application to global warming, *Geophys. Res. Lett.* 36 (2009) L16706.
- [23] N.M. Yuan, Z.T. Fu, J.Y. Mao, Different scaling behaviors in daily temperature records over China, *Physica A* 389 (2010) 4087–4095.
- [24] E. Koscielny-Bunde, A. Bunde, S. Havlin, Y. Goldreich, Analysis of daily temperature fluctuations, *Physica A* 231 (1996) 393–396.
- [25] A. Kiraly, I. Bartos, I.M. Janosi, Correlation properties of daily temperature anomalies over land, *Tellus A* 58A (2006) 593–600.
- [26] G. Vattay, A. Harnos, Scaling behavior in daily air humidity fluctuations, *Phys. Rev. Lett.* 73 (1994) 768–771.
- [27] Guangxing Lin, Xi Chen, Zuntao Fu, Temporal-spatial diversities of long-range correlation for relative humidity over China, *Physica A* 383 (2007) 585.
- [28] B. Podobnik, P.C. Ivanov, K. Biljakovic, D. Horvatic, H.E. Stanley, I. Grosse, Fractionally integrated process with power-law correlations in variables and magnitudes, *Phys. Rev. E* 72 (2005) 026121.
- [29] J.W. Kantelhardt, S.A. Zschiegner, E. Koscielny-Bunde, S. Havlin, A. Bunde, H.E. Stanley, Multifractal detrended fluctuation analysis of nonstationary time series, *Physica A* 316 (2002) 87–114.
- [30] Guangxing Lin, Zuntao Fu, A universal model to characterize different multi-fractal behaviors of daily temperature records over China, *Physica A* 387 (2008) 573–579.
- [31] B. Podobnik, H.E. Stanley, Detrended cross-correlation analysis: a new method for analyzing two nonstationary time series, *Phys. Rev. Lett.* 100 (2008) 084102.
- [32] W.-X. Zhou, Multifractal detrended cross-correlation analysis for two nonstationary signals, *Phys. Rev. E* 77 (2008) 066211.
- [33] B. Podobnik, D. Horvatic, A.M. Petersen, H.E. Stanley, Cross-correlations between volume change and price change, *PNAS* 106 (2009) 22079.
- [34] B. Podobnik, I. Grosse, D. Horvatic, S. Ilic, P.Ch. Ivanov, H.E. Stanley, Quantifying cross-correlations using local and global detrending approaches, *Eur. Phys. J. B* 71 (2009) 243.
- [35] D. Horvatic, H.E. Stanley, B. Podobnik, Detrended cross-correlation analysis for non-stationary time series with periodic trends, *Europhys. Lett.* 94 (2011) 18007.
- [36] Y. Ashkenazy, P.Ch. Ivanov, S. Havlin, C.K. Peng, A.L. Goldberger, H.E. Stanley, Magnitude and sign correlations in heartbeat fluctuations, *Phys. Rev. Lett.* 86 (2001) 1900–1903.
- [37] Y. Ashkenazy, S. Havlin, P.Ch. Ivanov, C.K. Peng, V. Schulte-Frohlinde, H.E. Stanley, Magnitude and sign scaling in power-law correlated time series, *Physica A* 323 (2003) 19–41.
- [38] Y. Ashkenazy, D.R. Baker, H. Gildor, S. Havlin, Nonlinearity and multifractality of climate change in the past 420, 000 years, *Geophys. Res. Lett.* 30 (2003) 2146.
- [39] R.N. Mantegna, H.E. Stanley, Scaling behavior in the dynamics of an economic index, *Nature* 376 (1995) 46–49.
- [40] T. Kalisky, Y. Ashkenazy, S. Havlin, Volatility of linear and nonlinear time series, *Phys. Rev. E* 72 (2005) 011913.
- [41] R.B. Govindana, A. Bunde, S. Havlin, Volatility in atmospheric temperature variability, *Physica A* 318 (2003) 529–536.
- [42] I. Bartos, I.M. Jnosi, Nonlinear correlations of daily temperature records over land, *Nonlinear Process. Geophys.* 13 (2006) 571–576.
- [43] G. Wang, A.J. Dolman, R. Blender, K. Fraedrich, Fluctuation regimes of soil moisture in ERA-40 re-analysis data, *Theor. Appl. Climatol.* 99 (2010) 1–8.
- [44] K. Hu, P.Ch. Ivanov, Z. Chen, P. Carpena, H.E. Stanley, Effect of trends on detrended fluctuation analysis, *Phys. Rev. E* 64 (2001) 011114.
- [45] B. Podobnik, D. Horvatic, A.L. Ng, H.E. Stanley, P.Ch. Ivanov, Modeling long-range cross-correlations in two-component ARFIMA and FIARCH processes, *Physica A* 387 (2008) 3954–3959.
- [46] T. Schreiber, A. Schmitz, Surrogate time series, *Physica D* 142 (2000) 346–382.
- [47] T.W. Anderson, D.A. Darling, Asymptotic theory of certain “goodness-of-fit” criteria based on stochastic processes, *Ann. Math. Stat.* 23 (1952) 193–212.
- [48] M.A. Stephens, EDF statistics for goodness of fit and some comparisons, *J. Amer. Statist. Assoc.* 69 (1974) 730–737.
- [49] D. Rybski, A. Bunde, On the detection of trends in long-term correlated records, *Physica A* 388 (2009) 1687.
- [50] H.A. makse, S. Havlin, M. Schwartz, H.E. Stanley, Method for generating long-range correlations for large systems, *Phys. Rev. E* 53 (1996) 5445.